International Journal of Refrigeration 175 (2025) 118–127

Contents lists available at ScienceDirect

International Journal of Refrigeration

journal homepage: www.elsevier.com/locate/ijrefrig

INSTITUT INTERNATIONAL DU FROID
INTERNATIONAL INSTITUTE OF REFRIGERATION

Compressor-assisted heat transformer for low-grade heat recovery

Tommaso Toppi *, Gianluca Abrami, Marcello Aprile

Department of Energy, Politecnico di Milano, 20156 Milano, Italy

ARTICLE INFO

Keywords:
Compression heat transformer
Waste heat recovery
Temperature upgrade
District heating
Industrial steam
Heat recovery from data center

ABSTRACT

The recovery of low-temperature waste heat can be promoted by upgrading its temperature. Heat transformers can increase the temperature of a heat stream while using little electrical energy, at the price of rejecting part of the heat input to a lower temperature sink. However, the lifting capability of heat transformers are limited by the operating conditions and often insufficient to meet the temperature requirements of many applications. An option to overcome this limitation is to use a compressor-assisted heat transformer (CHT), which benefits from the mechanical work of a compressor to expand the lifting capability. This work analyzes two alternative variation of CHT, characterized by a different positioning of the compressor in the thermodynamic cycle: CHTa, with the compressor at low pressure and CHTb with the compressor at high pressure. The CHTb variation showed higher electrical efficiencies (in the range 5–15 vs 1.5–10) and lower maximum compressor temperature (180 vs. 230 °C) than the CHTa, when recovering heat at 60 °C to deliver upgraded heat up to 120 °C. The use of the CHTb is therefore further investigated in four practical applications, assuming heat recovery from data centers, combined heat and power plants, district heating networks and industrial steam as a high temperature sink. In all the applications the CHTb has a higher electrical COP than the one of a reference heat pump, with values ranging from 4.5 to >25.

1. Introduction

Enhancing waste heat recovery is considered one of the crucial action to meet the emission reduction targets. Many efforts have already been made to exploit available waste heat into processes or applications with matching temperature and nowadays high and medium temperature waste heat are often recovered directly in the industrial processes (Hackl et al., 2011), to power district heating networks (Moser and Lassacher, 2020), or for electricity generation with organic Rankine cycles (Loni et al., 2021). However, a significant amount of waste heat at temperatures below 100 °C exists but, being rarely monitored and often de-centralized, it is not exploited. Waste heat below 100 °C comes from electricity generation, petrochemicals, refineries, cement production, food processing, pulp and paper sector, datacenters, wastewater treatment. electrical systems, water resources, refrigeration systems, and heat from underground railways (Rattner and Garimella, 2011; Luberti et al., 2022). Even if a comprehensive identification and quantification of the actual availability of low-temperature waste heat is not available, studies suggest that it is not negligible. As an example, it is estimated that for the UK these sources could overcome the needs for heating in the country, even if the amount of heat which can be economically recovered is uncertain (Davies et al., 2023).

District heating is often considered a key option in the process of decarbonizing the heating sector, thanks to its capability to both establish energy communities characterized by high renewable penetration and to match availability of waste heat with heating demand. The use of low-grade waste heat in a district heating network could represent an interesting option both from the economic and the environmental point of view. This is strengthened by the fact that low-temperature waste heat is often generated relatively close to the urban areas, as in the case of datacenter (Ebrahimi et al. 2014). Low-temperature networks are well suited to enable direct waste heat recovery however, many existing networks are designed to operate at higher temperatures and a reduction of their operating temperature would impact both their capacity and their capability to serve high-temperature users.

Temperature enhancement of low-temperature waste heat can enable heat recovery both within the industry and towards district heating networks. A first option to achieve this goal is the use of vapor compression heat pumps. However, their potential is limited by the low efficiency at high thermal lifts, which leads to high electricity consumption when a large difference exists between the available waste heat and the required temperatures (Arpagaus et al., 2018). A second

* Corresponding author.
E-mail address: tommaso.toppi@polimi.it (T. Toppi).

https://doi.org/10.1016/j.ijrefrig.2025.03.045
Received 12 September 2024; Received in revised form 7 February 2025; Accepted 28 March 2025
Available online 29 March 2025

Nomenclature

C	ammonia mass fraction, -
COP	coefficient of performance, -
CR	compression ratio, -
Q	heating capacity, kW
P	pressure, kPa
T	temperature, °C
v	specific volume, $m^3\ kg^{-1}$
V_Q	vapor volume per unit of absorber heat, $m^3\ MJ^{-1}$
W	mechanical power, kW

Acronyms and abbreviations

ABS	absorber
CHP	Compressor Heat Transformer
CMP	compressor
COND	condenser
EVA	evaporator
GEN	generator
PMP	pump
RHX	refrigerant heat exchanger
SHX	solution heat exchanger

Greek letters

Δ	difference
ε_Q	heat recovery efficiency

Subscripts

CT	cooling tower
DC	data center
DES	desalination
DH	district heating
COG	cogenerator
GW	ground water
H	high temperature circuit
HR	heat rejection
HP	heat pump
HT DH	high-temperature district heating
L	low temperature circuit
LT DH	low-temperature district heating
M	intermediate temperature circuit
WH	waste heat
el	electrical
inl	inlet
max	maximum
out	outlet
poor	solution poor in ammonia
rich	solution rich in ammonia
th	thermal

possibility is the use of a heat transformer, which has the advantage of requiring a small amount of electricity, but it experiences limitations in terms of working range. In particular, the lifting capability is influenced by the low temperature availability of the cold sink for the heat rejection (Garone at al. 2017). Furthermore, when H_2O-LiBr is employed as the working pair, as is the case in the majority of heat transformers manufactured, the advantages of a potentially accessible cold sink in the vicinity of or below 0 °C cannot be capitalized due to the freezing of the water used as refrigerant. In addition, having a COP of about 0.45–0.50 (Cudok et al. 2021), a heat transformer lifts the temperature of about half of the driving heat, with the remaining half being rejected at lower temperature.

To overcome these limitations several alternative cycle configurations have been investigated.

With a double effect heat transformer (DE-HT) higher COP is achieved, although with a reduction of the lifting capability (Zhao et al. 2005). This is achieved by placing the externally heated generator at intermediate pressure and using the heat of condensation of the generated vapor for the desorption process in a low-pressure generator, at the same pressure of the condenser. With this solution the amount of vapor generated increases, with benefit for the COP, which can reach about 0.65. On the other hand, the maximum temperature lift is capped by the need of evaporating refrigerant at intermediate pressure.

Alternatively, the use of a double absorption configuration allows higher lifts, with the drawback of lower COP. The main idea behind most of the double absorption cycles is to introduce an intermediate pressure between the high and low pressures where, by means of an intermediate-pressure absorber, vapor is generated at higher temperature and pressure than the one allowed by the heat used to drive the heat transformer. A first cycle layout implementing this concept, called DAHT type 1 in (Ma et al. 2016), was presented by Rivera et al. (1994a) and showed the capability to upgrade heat from 80 °C to 152 °C with a COP of about 0.3. A second layout (Rivera et al., 1994b), called DAHT-2, presents a simpler configuration. In this case, the solution leaving the generator is entirely pumped at the high-pressure absorber, where it absorbs vapor releasing useful heat, before being split in two streams, one routed at the intermediate pressure absorber/high pressure evaporator and one laminated at low pressure. The DAHT-3 (Zhao et al. 2003a) is similar to the DAHT type 2, with the difference that the split is done on the poor solution before the high-pressure absorber, routing part of it at the intermediate pressure absorber/high pressure evaporator. This solution increases the temperature lift by 5–10 °C maintaining constant the COP. In a fourth configuration (DAHT type 4) by Mostofizadeh and Kulick, 1998, the split on the solution is avoided by routing the rich solution leaving the absorber entirely at intermediate pressure, where it is further enriched by the vapor from the evaporator and provides the heat for evaporating the refrigerant stream sent to the absorber. According to (Zhao et al., 2003b) this configuration has the highest COP among the other double absorption configurations, especially when a large temperature lift is needed. These cycles are more complex than single stage heat transformers and experience COP degradation due to the strategy deployed to extend the temperature lift.

An option to keep the cycle simple and avoid COP degradation, while increasing the lifting capacity, is the use of a compressor. The addition of a compressor stage to a heat transformer can be achieved by thermally coupling a vapor compression heat pump to a heat transformer or by integrating a compressor directly into the heat transformer cycle. These systems are commonly referred to as Hybrid Compressor Absorption Heat Transformers (HCAHT), although the naming of the two options is not unique in the literature. The first system is also called Hybrid Absorption Compressor Heat Pump (HCAHP) (Gao et al., 2021a; Zhang et al. 2022), while the second is called Absorption Compression Heat Transformer (ACHT) (Zhou et al., 2024), Compression Assisted Heat Transformers (CAHT) (Gao et al., 2021a) or simply Compression Heat Transformer (CHT), as will be done in this paper. In either case, the resulting system combines the features of a heat transformer and a heat pump, exploiting the ability of the former to upgrade low temperature heat with the flexibility and additional lift capability provided by the mechanical compressor of the latter. From an operational point of view, the price to be paid for this additional flexibility is the electrical consumption of the compressor. It is therefore necessary to assess the efficiency of the system on both a thermal and an electrical basis.

In an HCAHP system where the two sub-cycles are thermally coupled by internal heat transfer, the vapor compression cycle is used to upgrade

the waste heat used in the generator and evaporator of a classic absorption heat transformer. This can be done in either a series (Zhang et al. 2022) or parallel (Gao et al., 2021b) configuration. In the first case, the refrigerant leaving the compressor is first sent to the generator and then to the evaporator of the heat transformer. In the latter case, the compressed refrigerant is split into two branches and routed in parallel to the two heat exchangers. In both cases, internal heat recovery is performed by transferring heat from the condenser of the heat transformer to the evaporator of the compression heat pump, reducing the need for external low-temperature heat and the size of the heat exchanger used as the evaporator. The concept can be further extended to increase the system's lifting capacity by adding a third stage. This can be achieved using either a single stage heat pump with a double stage heat transformer or a double stage heat pump with a single stage heat transformer (Zhang et al., 2022). The latter configuration was found to have the highest lifting capacity, upgrading heat at 181 °C with a COP of 1.32 at a source temperature of 30 °C. This is significantly higher than the two-stage options, which showed a maximum thermal lift of 160 °C and a COP of 1.1 under the same conditions.

For the CHT, studies on both adsorption and absorption cycles can be found. For what concerns the former Jang et al., 2020 studied a hybrid resorption-compression heat transformer with both heat storage and temperature upgrading functions. In this system, the compressor is used both in the charging phase, to reduce the desorption temperature and in the discharging phase to increase the outlet temperature. When considering a CHT based on an absorption heat transformer, two options are available. In fact, a compressor can be added either between the generator and the condenser to allow a higher condensation temperature, or between the evaporator and the absorber to increase the pressure in the latter component and the temperature of the useful heat. In this work, the two configurations are referred to by the abbreviations CHTa and CHTb respectively. The former option has been proposed in (Wang et al. 2018), which studied its application for space heating in some cities in the northern part of China, assuming waste energy available at 12 °C and useful heat delivered at 45 °C. The comparison with water- and air-sourced vapor compression heat pumps showed that the compressor assisted heat transformer requires up to 25 % and 57 % less electricity on annual basis respectively, with higher savings in the colder regions. The latter option, exploiting the compressor between the evaporator and the absorber, was investigated by (Wang et al., 2017) for a similar application, using very low temperature waste heat ($T \approx 15$ °C), rejecting heat toward a very low ambient temperature ($T < -10$ °C) and providing heat for low temperature heating ($T \approx 45$ °C). The CHTb proved to require lower electrical input than a water source heat pump operating at the same conditions. Both studies focuses on the use of a compression assisted heat transformer for space heating in a cold environment while recovering low temperature heat. A different range of working conditions has been considered by Zhou 2024, which used CHTb for the production of heat up to 150 °C for industrial uses, while recovering heat below 100 °C. Unlike the previous studies, they used water-lithium bromide as working pair with the purpose of limiting the pressures. Additionally, they introduced the injection of liquid refrigerant in the compression chamber to limit the superheating at the compressor outlet. From the presented results, an electrical COP (ratio between upgraded heat and electrical input) of about 5 can be derived when the waste heat temperature is 90 °C, the heat rejection temperature 25 °C and the upgraded heat is delivered at 153 °C.

These works suggest that the addition of a compression stage can effectively increase the lifting capacity of a heat transformer. With regard to CHT systems where the compressor is installed directly in the absorption cycle, the available literature is still incomplete. In particular, an exhaustive comparison of the two cycle options under the same conditions is not available. Gao 2021b mentions that the option with the compressor located between the evaporator and the condenser requires more compression work for the same pressure ratio due to the superheated vapor at the compressor inlet. In addition, when water-lithium bromide is used as the working fluid pair, this configuration has a higher risk of crystallization due to the higher salt concentration. However, the risk of crystallization can be avoided by using the ammonia-water solution as the working fluid. In addition, a more interesting comparison could be made using the same operating conditions rather than the same compression ratio.

For this reason, the present work focuses on the study of CHT with the aim of determining the most suitable configuration for applications characterized by the recovery of heat below 100 °C to provide upgraded heat for industrial or district heating uses, and at the same time to outline the characteristics and potential of these cycles. Ammonia-water is used as the working fluid because, although it presents some challenges for the design of the compressor, this pair doesn't have to face problems of crystallization and has the advantage of compactness.

After presenting the modelling approach, the two cycle variants CHTa and CHTb are compared numerically to assess which is the most appropriate for the selected temperature ranges, providing an insight into the two thermodynamic cycles and highlighting the differences between them. The effect of compressor discharge pressure on cycle efficiency is also analyzed. Finally, the operation of the most promising cycle is studied for specific applications typical of district heating networks and the industrial sector. The electrical efficiency is compared with that of a vapor compression heat pump, which is the main competitor of the CHT in these specific applications.

2. Cycles layout

In the basic heat transformer absorption cycle, the heat input is supplied to evaporator (EVA) and generator (GEN), the useful heat is generated at the absorber (ABS), and the discarded heat is generated at the condenser (COND). Two options are available when adding a compressor to a single stage heat transformer. In the former, called CHTa in this work and represented in Fig.1a, the compressor (CMP) is installed between the generator and the condenser, allowing the condensation pressure to be higher than the generation pressure. Alternatively, in the CHTb cycle (see Fig 1b), the compressor is installed between the evaporator and the absorber, allowing the evaporation pressure to be lower than the absorption pressure. In both cases the use of the compressor extends the working range of the heat transformer, enabling the use of heat sources (for GEN and EVA) at lower temperatures or heat sinks (for COND and ABS) at higher temperatures.

In both cycles, two internal heat exchangers are used for heat recovery purposes: the refrigerant heat exchanger (RHE) and the solution heat exchanger (SHX).

The employed working fluid is ammonia-water, which has been shown in Garone at al. (2017) to be a suitable pair for absorption heat transformers, allowing high efficiency and compact design, while not posing significant corrosion problems in the working conditions considered in this work.

It must be noted that for both cycles, the ammonia mass fraction in the solution loop (solid lines in Fig. 1) is linked to the compression ratio once the temperatures at the external heat exchangers are set. Consequently, the available degree of freedom provided by the cycle is the compressor inlet pressure for the CHTa cycle and the compressor outlet pressure for the CHTb cycle.

3. Modelling approach

The two alternative cycles were built assuming that all heat exchangers have a counter current configuration. In the generator, a phase separator is added at the solution outlet, where a tray column is placed on the vapor stream and used to increase the ammonia mass fraction. In the absorber, vapor and poor solution are adiabatically mixed at the inlet of the heat exchanger.

The following modelling assumption were also made:

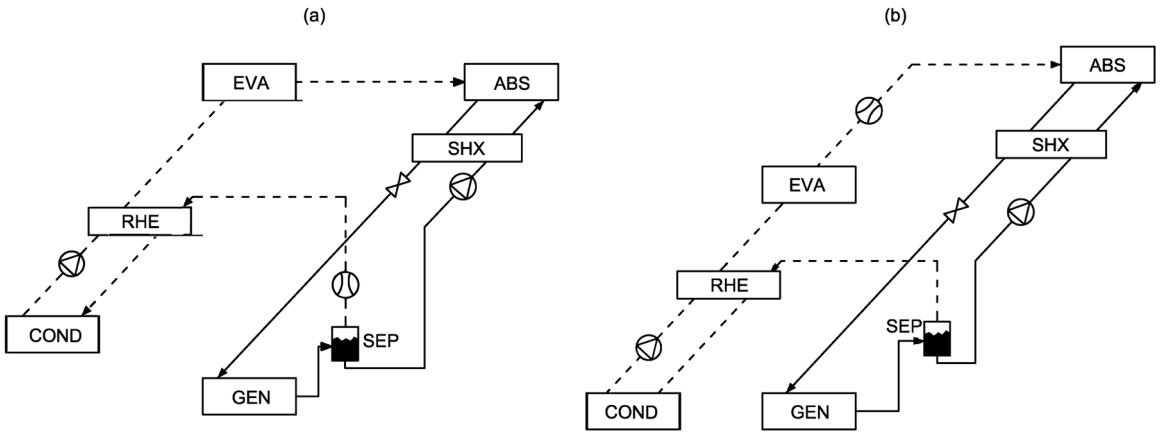

Fig. 1. Cycle layout: CHTa (a) and CHTb (b).

- Pressure losses are negligible in the pipes and in all heat exchangers (Xu and Wang, 2018; Gao 2021a) but the absorbers, where a fixed value of 20 kPa is assumed (Toppi et al. 2017).
- Throttling is isenthalpic (Xu and Wang, 2018; Gao 2021a).
- Heat losses are negligible (Gebreslassie et al., 2010; Zhang 2022).
- The effectiveness of the internal heat exchangers (SHX and RHE) is 0.85.

The numerical model of the cycles has been built using STACY (Aprile et al., 2018) as mathematical framework for steady-state simulation of absorption cycles, which has been extensively validated for ammonia-water absorption cycles. The tool is based on a modular approach and supports the creation of the system of algebraic equations, containing mass, species, and energy balances for each domain based on the flow rates and thermodynamic states at its ports. Being N_p the number of ports of a domain, the balance equations are described by Eq. (1)-3.

$$\sum_{p=1}^{N_p} \dot{m}_p = 0 \tag{1}$$

$$\sum_{p=1}^{N_p} \dot{m}_p X_p = 0 \tag{2}$$

$$\sum_{p=1}^{N_p} \dot{m}_p h_p + Q_{in} + W_{in} = 0 \tag{3}$$

Redundant equations are deleted, and the system is completed with heat transfer relationships, auxiliary conditions such as mass flow rates, independent species mass fractions, pressure levels and outlet temperatures of external circuits. In particular, the auxiliary conditions at the absorber, condenser and evaporator are imposed based on the following assumptions:

- In the generator, a saturation condition is set for the liquid and vapor leaving the phase-separator and a minimum pinch of 5 °C is set at the heat exchanger between hot water and solution (Xu and Wang, 2018).
- At the absorber, a fixed subcooling of 1 °C at the solution outlet and minimum temperature difference of 5 °C is imposed along the heat exchanger (Toppi et al. 2016).
- In the condenser, a fixed subcooling of 1 °C is imposed at the refrigerant outlet and the minimum temperature difference of 3 °C is imposed between the refrigerant and the cooling water (Toppi et al. 2016).
- In the evaporator, the minimum temperature difference between the heat source fluid and the refrigerant is 3 °C and the refrigerant leaves the heat exchanger with a vapor quality of 0.95 (Garone et al., 2017).

The properties of the water-ammonia solution have been derived from Ziegler and Trepp (1984) for pressures below 50 bar and from Ibrahim and Klein (1993) for pressures above 50 bar.

This modelling approach has the advantage that the calculation is not related to a specific machine with given components and size, but that the cycle can be adapted to any conditions while maintaining the same design principles. This makes the results more comparable and easier to generalise.

Following a similar criterion, the mass flow of the external circuits has been adjusted to maintain fixed temperature differences, depending on the application:

- Generator and evaporator are connected in series and an total temperature difference between generator inlet and evaporator outlet (ΔT_M) is set.
- A temperature difference of ΔT_H is set between the inlet and outlet of the absorber.
- A temperature difference of ΔT_C is set between the condenser inlet and outlet.

The cycle performances are evaluated on the basis of the electrical COP, defined as in Eq. (4), which gives the ratio between the heating capacity released at high temperature and the electrical power needed to operate the compressor and the refrigerant and solution pumps. The electrical power is calculated assuming an efficiency of the electric motors of 0.9 (Zhou et al., 2024) and isentropic pump and compressor efficiencies of 0.8 and 0.7, respectively (Gao et al., 2021a).

$$COP_{el} = \frac{Q_{ABS}}{W_{COMP} + W_{P\ REF} + W_{P\ SOL}} \tag{4}$$

Moreover, the thermal COP, defined in Eq. (5), expresses the ratio between the heating capacity at high temperature and the heating power at intermediate temperature provided to the cycle. It is worth mentioning that, for the CHT, COP_{th} does not strictly represent the share of the driving heat which is upgraded to a higher temperature, since in the energy balance the contribution of the compressor is also included. Thus, to consider the efficiency of the heat transformation process alone, the correct performance indicator is ε_Q, defined as the fraction of the heat input at intermediate temperature which is upgraded at high temperature net of the compressor work (see Eq. (6)).

$$COP_{th} = \frac{Q_{ABS}}{Q_{GEN} + Q_{EVAP}} \tag{5}$$

$$\varepsilon_Q = 1 - \frac{Q_{COND}}{Q_{GEN} + Q_{EVAP}} \quad (6)$$

4. Results

Before using the model to explore the potential of the compressor-assisted heat transformers in various applications, a comparison of the results with the ones presented in Wang et. al (2018) was performed. Once verified the consistency of the results, a wide range of working conditions was explored with the purpose of investigating the impact on the cycle of the pressures set by the compressor, i.e. the low pressure in the CHTa and the high pressure in the CHTb. Finally, the use of the two cycles is explored for working conditions corresponding to specific applications.

4.1. Validation of the model

At first the alignment of the model with the data available in the literature is verified. The results of the numerical model used for this study are compared with the ones provided in Wang et. al (2018) for the CHTb.

In the former work, the driving temperature was 10 °C, the heat rejection temperature −10 °C and upgraded heat temperature 45 °C, with a compression ratio of 2.0. Under these conditions, the primary energy efficiency was 0.42 i.e., 4.5 % lower than the value 0.44 obtained from the model used within this work.

More information for a comparison are available in the latter study, where the CHTb is used to recover very low temperature heat ($T_{M\ in}/T_{M\ out}$ = 15.00/11.75 °C), with discharge temperature typical of the winter conditions in cold climates ($T_{L\ in}/T_{L\ out}$ = −15.00/−9.65 °C) to provide heat to a low-temperature district heating network ($T_{H\ in}/T_{H\ out}$ = 41.75/45.00 °C), with a ratio between high and intermediate pressure of 2.

Running the numerical model used in this study under the same conditions, very similar results are obtained (see Table 1). Differences around 5 % are found for COP_{el} and COP_{th}, and pressures and mass fractions are close, except for the low-pressure, which in turns influences the concentration of the poor solution.

These differences can be explained with the slightly different hypothesis of the two models (e.g. different pinch at the heat exchangers) and in the use in this work of a tray column after the generator, which was not necessary in very low-temperature applications.

4.2. Comparison between the two CHT configurations

In this section the two cycles layout of the CHT are compared in terms of COP_{el}, COP_{th}, ε_Q and compressor outlet temperature, under given conditions. For each condition the contribution of the compressor is changed, exploiting the degree of freedom it provides in the CHTa to lower the pressure at the generator (P_L) with respect of the condensation pressure (P_M) and to increase the absorber pressure (P_H) compared with the evaporation pressure (P_M) in the CHTb.

For the comparison the following conditions were used:

Table 1
comparison of the model results with the ones from a previous study.

	Wang et. al (2018)	This work	Difference
COP_{el}	6.8	7.1	4.4 %
COP_{th}	0.497	0.468	−5.8 %
P_H (bar)	12.10	12.06	0.04
P_M (bar)	6.07	6.03	0.04
P_L (bar)	3.65	3.19	0.46
C_{poor} (-)	0.65	0.61	0.04
C_{rich} (-)	0.69	0.69	0.00

- Heat source inlet temperature ($T_{M\ in}$) of 60 °C, with a temperature difference ΔT_M of 10 °C.
- Condenser inlet temperature ($T_{L\ in}$) of 0 °C with a temperature difference ΔT_L of 5 °C.
- Absorber outlet temperature ($T_{H\ out}$) ranging from 90 °C to 120 °C, with a difference between supply and return (ΔT_H) of 30 °C, resulting in inlet temperatures from 60 °C to 90 °C.

A range of different values of absorber outlet temperatures was explored for the CHTa, as shown in Fig. 2, where the values of COP_{th} (Fig. 2a), COP_{el} (Fig. 2b), ε_Q (Fig. 2c) and $T_{CMP\ out}$ (Fig. 2d) are reported as function of the compressor inlet pressure (P_L). In the charts, each line corresponds to an absorber outlet temperature and the bullet of the corresponding color indicates the position of the maximum of the COP_{el}, except for Fig. 2b, where the bullets indicate the maximum of the COP_{th}. The upper limit of the explored pressure range is given by the maximum value which allows the CHT to operate under the given conditions, while the minimum value was chosen paying attention to include the range where the maximum COP_{el} is found and excluding excessively low value, with no relevance. The COP_{th} increases monotonically when the inlet pressure is lowered, meaning that the higher the pressure difference across the compressor, the higher the output at the absorber (Q_H) compared with the input at the evaporator and generator (Q_M). However, the increase of Q_H is mainly due to the higher energy input required at the compressor, which is useful mechanical power rather than recovered waste heat. For this reason, ε_Q, which represents a better indicator to express the capability to make good use of the waste heat, experiences a maximum at a given level of P_L and decreases if the pressure is further lowered. A maximum is also found for the COP_{el} (see Fig. 2b), positioned at a slightly lower pressure than the maximum which allows the cycle operation. This is the condition which is most likely selected when operating a CHT in those cases when the input is waste heat and the electricity is more valuable. Tuning the CHTa to maximize the COP_{el} results in ε_Q between 0.32 and 0.43, dependent on the absorber temperature and rather close to the respective maximum values. A further reason in favor of limiting the reduction of P_L is the compressor outlet temperature, which increases with the compression ratio. As can be seen from Fig. 2d, the compressor outlet temperature can rise to 300 °C, a value not compatible for most of the standard compressors. Instead, operating at the low pressure level which maximize the COP_{el}, the compressor outlet temperature is limited at 230 °C, a value closer to the operating range of the compressors used for high temperature heat pumps.

Replicating the study for the CHTb, the results reported in Fig. 3 are found. With this cycle, the charts are plotted against the compressor outlet pressure ($P_{CMP\ out}$), i.e., P_H. In this case, the range of pressure which is explored has the minimum pressure which enables the cycle operation as the lower limit. Instead, the upper limit is selected to include the relevant operating conditions, excluding higher pressure levels, potentially feasible but progressively less convenient in terms of performances.

At P_H above the lower limit, after a first increase of the COP_{th}, the curves become substantially flat (see Fig. 3a), unlike what was observed for the CHTa. Moreover, the plateau of the COP_{th} is practically independent on the absorption temperature, being located in the narrow range 0.48–0.53. Consequently, if the compression pressure outlet is set to maximize the COP_{el}, the resulting COP_{th} is also very close to its maximum value. The same can also be said for ε_Q (chart in Fig. 3c), which values are within the range 0.43–0.47, rather close to the COP_{th} and with just a slightly reduction as the absorber temperature increases. The temperatures at the compressor outlet depend mainly on P_H and are comprised in a range between 100 °C and 180 °C if the cycle is operated to maximize the COP_{el} (see Fig. 3d).

Comparing the graphs in Fig. 2 and Fig. 3 side by side, a higher COP_{th} can be observed for the CHTa than for the CHTb. However, as discussed, this is due to the higher energy supplied by the compressor rather than

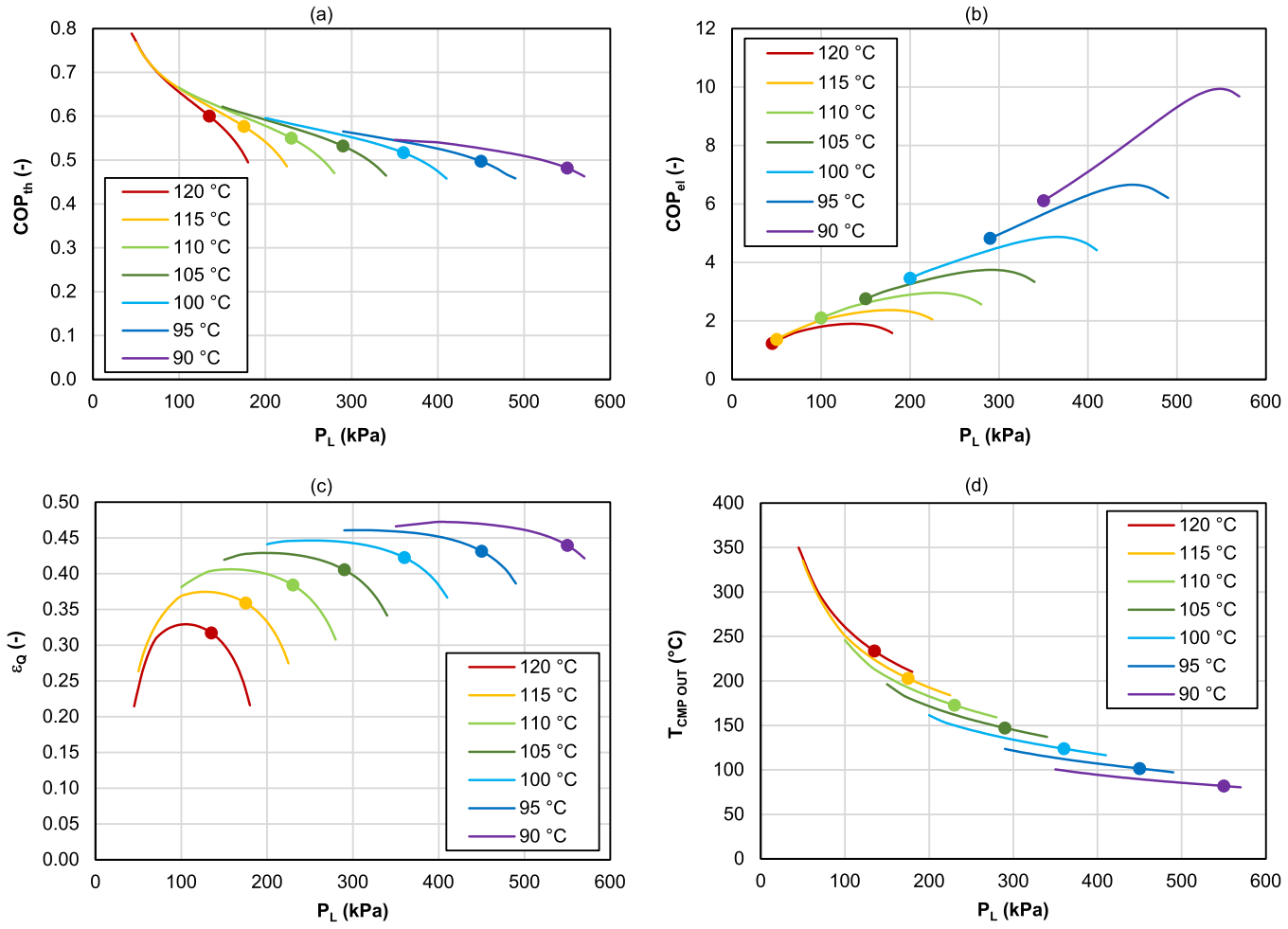

Fig. 2. Performances of the CHTa as function of the $P_{CMP\ inl}$ for $T_{H\ out}$ ranging from 100 to 130 °C, with $T_{C\ in}$ = 0 °C and $T_{M\ in}$ = 60 °C.

to a more efficient heat transformation process. In fact, considering the ε_Q as an indicator, higher and more constant values can be found for CHTb than for CHTa. In addition, the COP_{el} is higher for the CHTb in all the operating conditions studied.

The main reason for these differences is the different location of the compressor. In fact, since it takes place at low pressure, the compression process in the CHTa is penalized by the higher specific volume of the inlet vapor. As can be seen in Fig. 4, where the specific volume (solid lines) is plotted ad a function of the outlet absorption temperature for the pressure that maximizes the COP_{el}, values in the range 0.27–1.1 m^3/kg are found for the CHTa and in the range 0.07–0.08 m^3/kg for the CHTb. The higher specific volume results in a higher V_Q, i.e. the volume of vapor passing through the compressor per unit of heat delivered by the absorber (dashed lines). This is only partially compensated for by the different pressure difference between the compressor inlet and outlet (ΔP_{CMP}), which ranges between 1 and 4 bar for the CHTa and from 5 to 30 bar for the CHTb, as shown in Fig. 5.

Another consequence of the different position of the compressor in the two cycles is that in the CHTb the energy associated with the superheating of the vapor resulting from the compression process can be converted directly into useful heat at high temperature in the absorber, whereas in the CHTa it is rejected at the condenser. The presence of the RHE mitigates this effect by cooling the vapor after the compressor and using this energy to pre-heat it before the evaporator. However, this reduces the load on the condenser and at the evaporator, which benefits the COP_{th}, but has little effect on the COP_{el}.

Fig. 5 also shows the compression ratio (CR), which is around 1.5 for both the configurations for the lower value of the absorber outlet temperature (90 °C). However, at higher absorber temperatures it increases more rapidly in the CHTa than in the CHTb, due to the very low pressure required at the generator in the first configuration.

Based on the analysis, the CHTb configuration looks more promising for practical applications due to the higher COP_{el} and lower temperature at the compressor outlet. In addition, while lower pressures are found for CHTa, when CHTb is operated to maximize COP_{el}, the maximum pressure P_H remains below 50 bar, a value that does not pose significant design or manufacturing challenges. For these reasons, the CHTb configuration has been used in the following section where the performance of the CHT is verified under some specific operating conditions.

4.3. Cases study

This section presents some case studies where the compression-assisted heat transformer can be successfully applied. The analysis is based on the CHTb, which was found to be the most promising configuration in terms of performance and compressor operating conditions. The following applications are studied:

1. High temperature district heating (DH) network driven by data center (DC) waste heat with ground water (GW) for heat rejection. Different temperature levels have been explored for the waste heat, assuming both water and air cooled data centers, and for the district heating, with temperatures chosen based on low, medium and high temperature networks..
2. Steam generation at 3 bar for an industrial process driven by waste heat from a CHP plant, with condensation heat rejected through a

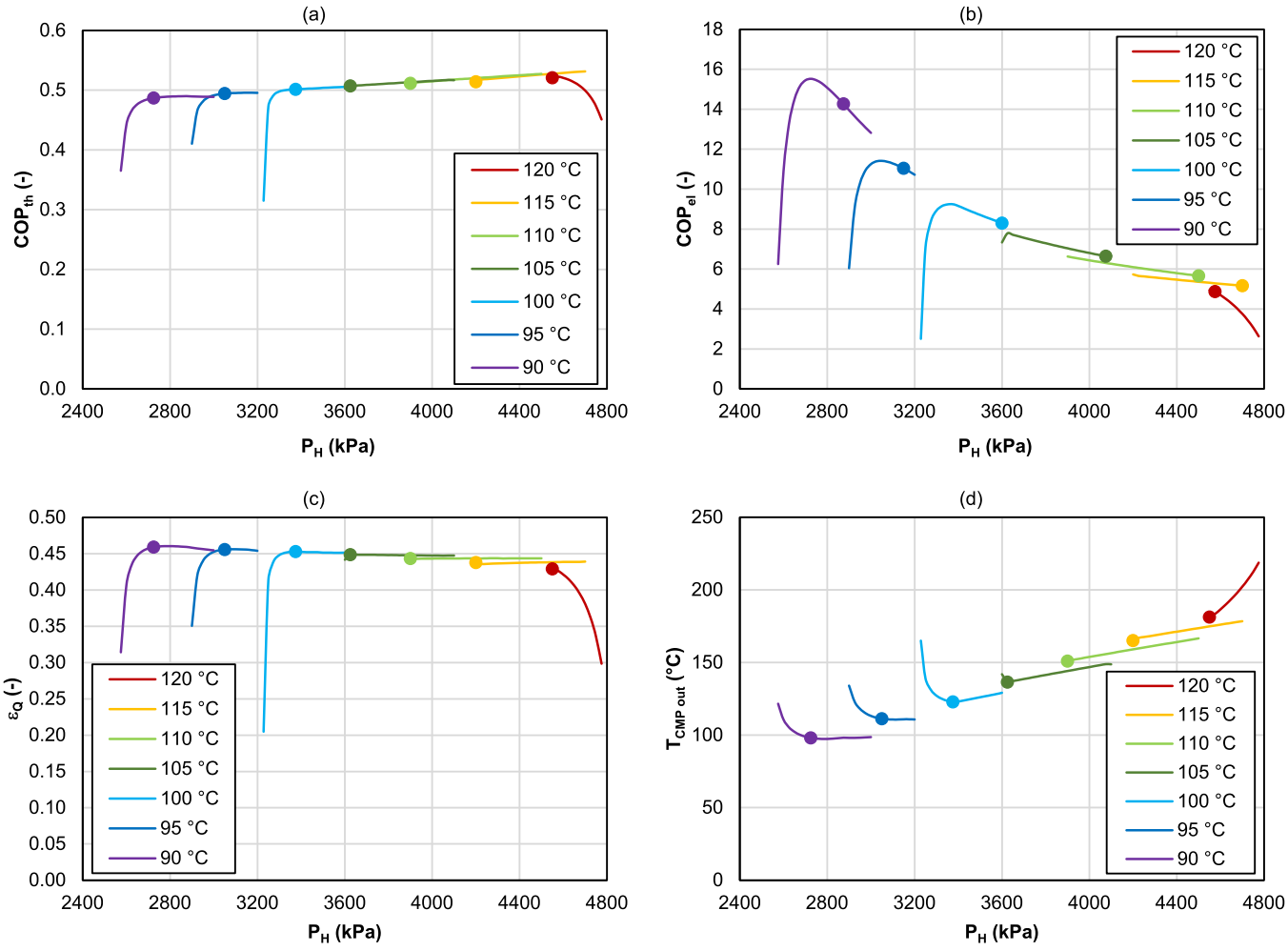

Fig. 3. Performances of the CHTb as function of the $P_{CMP\ inl}$ for $T_{H\ out}$ ranging from 100 to 130 °C, with $T_{C\ in}$ = 0 °C and $T_{M\ in}$ = 60 °C.

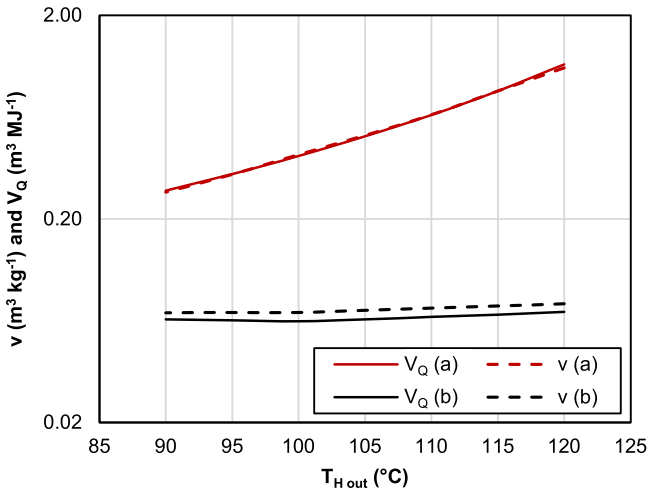

Fig. 4. Specific volume at the compressor inlet and specific compression energy.

cooling tower. The cases are differentiated through different heat rejection temperatures, simulating different climatic conditions.

3. Waste heat from a CHP plant used to simultaneously supply a high temperature (110/60 °C) and a low-temperature (65/35 °C) district heating networks. Different combinations are proposed using realistic temperatures for the three systems.
4. Waste heat driven desalination process with heat dissipation to the environment. The upgraded heat is used to evaporate water at 100 °C and four cases obtained by combining two waste heat temperatures and two heat rejection temperatures are proposed.

The schemes of the four case studies and the main results are shown in Fig. 6. In the table associated with each scheme, the source temperature (T_M), the heat rejection temperature (T_L) and the upgraded heat (T_H) are given as inlet/outlet for each case. The subscripts used in the figure refer to each specific case and indicates the source or the sink nature. For each condition, the calculated COP_{el} for the CHTb is given. For comparison, the COP corresponding to 60 % of the Carnot efficiency is also given, assuming that this is the maximum expected efficiency of a well-designed heat pump (Johra 2022).

The results show that the CHTb can be an interesting solution in the cases studied. As expected, high values of the heat source are advantageous for the COP_{el}, since the pressure increase required for the compressor is limited.

In the application of waste heat recovery from a data center and heat supply to a district heating network, the CHTb has a COP_{el} significantly higher than the reference vapor compression heat pump. Under the conditions considered, COP_{el} values between 6.3 and 12.5 were found, while the estimated values for a vapor compression heat pump would be between 3.8 and 5.8. This suggests that if the available waste heat temperature is properly matched to the temperature required by the

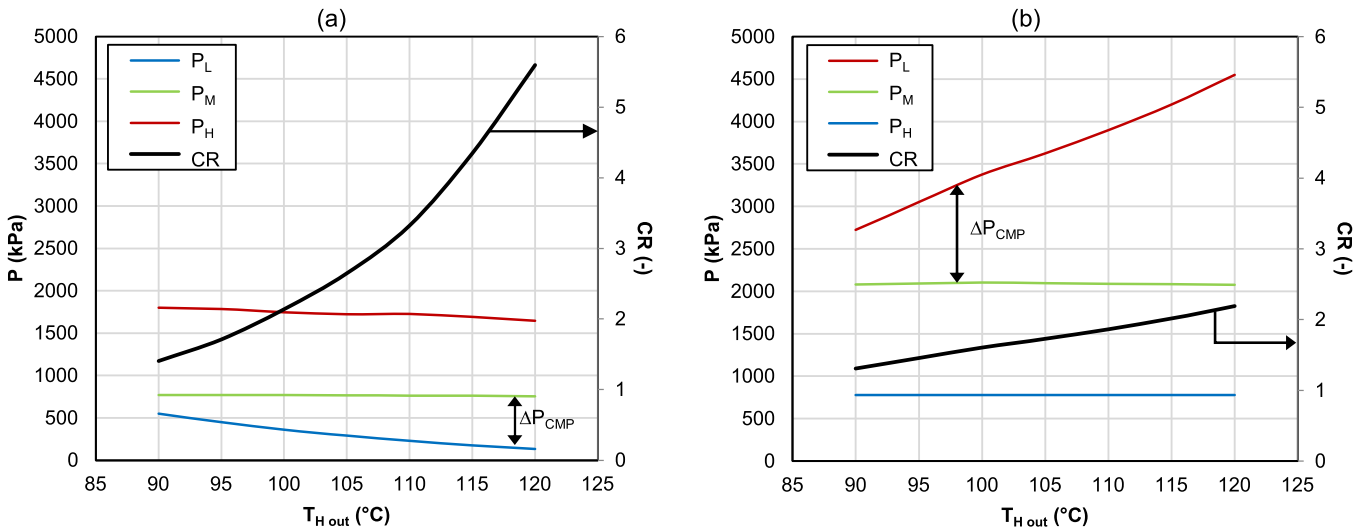

Fig. 5. Variation of the pressures and compressor ratio with T_H for the CHTa (a) and CHTb (b).

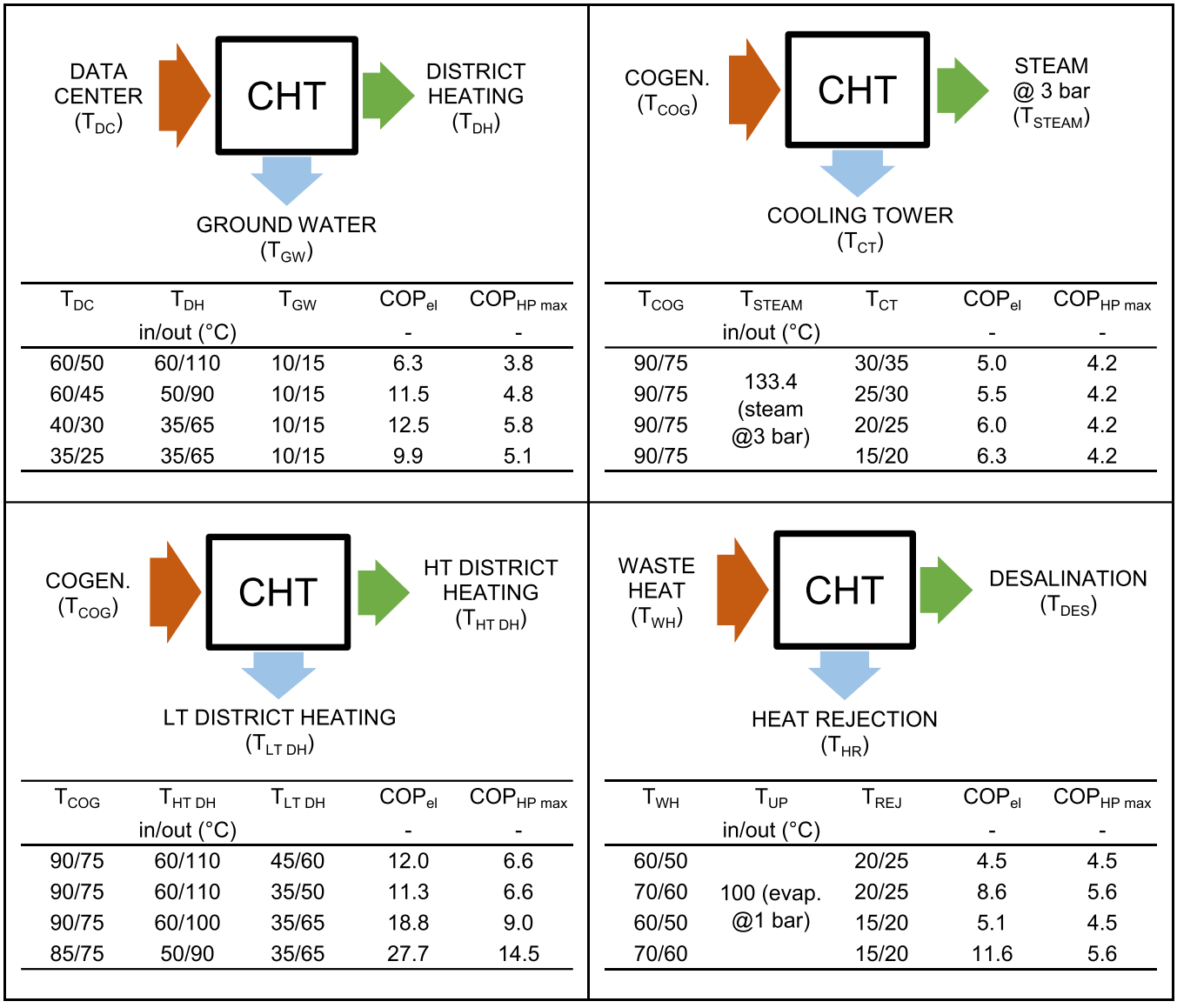

T_{DC}	T_{DH} in/out (°C)	T_{GW}	COP_{el} -	$COP_{HP\,max}$ -
60/50	60/110	10/15	6.3	3.8
60/45	50/90	10/15	11.5	4.8
40/30	35/65	10/15	12.5	5.8
35/25	35/65	10/15	9.9	5.1

T_{COG}	T_{STEAM} in/out (°C)	T_{CT}	COP_{el} -	$COP_{HP\,max}$ -
90/75	133.4 (steam @3 bar)	30/35	5.0	4.2
90/75		25/30	5.5	4.2
90/75		20/25	6.0	4.2
90/75		15/20	6.3	4.2

T_{COG}	$T_{HT\,DH}$ in/out (°C)	$T_{LT\,DH}$	COP_{el} -	$COP_{HP\,max}$ -
90/75	60/110	45/60	12.0	6.6
90/75	60/110	35/50	11.3	6.6
90/75	60/100	35/65	18.8	9.0
85/75	50/90	35/65	27.7	14.5

T_{WH}	T_{UP} in/out (°C)	T_{REJ}	COP_{el} -	$COP_{HP\,max}$ -
60/50	100 (evap. @1 bar)	20/25	4.5	4.5
70/60		20/25	8.6	5.6
60/50		15/20	5.1	4.5
70/60		15/20	11.6	5.6

Fig. 6. Schematization of the four possible applications of the CHTa and performances under four different operating conditions for each application.

district heating network, a CHT can provide significant savings over a heat pump for this type of application.

Similar results are found when waste heat from a CHP plant is used to simultaneously supply a low- and a high-temperature district heating network. In this case, the COP_{el} of the CHT ranges between 12 and 27.7, almost double that of a reference heat pump, which ranges between 6.6 and 14.5. Moreover, if the COP_{el} of the CHT is calculated including the heat rejected by the condenser and delivered to the low-temperature network, its values are more than double those shown in the table, making the solution even more interesting.

Better COP_{el} values for the CHT are also found in the two applications with steam production. However, the differences with the vapor compression heat pump are smaller. This is due to two independent factors:

- The two steam applications are characterized by a higher thermal lift, compared to the available driving temperature difference.
- In the absorber, the steam has a higher heat capacity than the solution absorbing the refrigerant vapor. As a result, in this heat exchanger the temperature pinch is on the solution outlet side rather than the solution inlet side, as in the case when the absorber is cooled by a liquid flow with lower heat capacity. This results in a poor temperature match between the two sides of the heat exchanger and in an increase in the high pressure.

However, in the case of steam production at 3 bar, the COP_{el} of the CHTb is in the range of 5.0–6.3, which is from 19 % to 50 % higher than the 4.2 calculated for the heat pump. For desalination, the same COP_{el} was found for the two technologies in the case of the higher heat rejection temperature, while in the case of the lower heat rejection temperature, the efficiency of the heat transformer was found to be about double that of the heat pump.

These results suggest a potential for the use of the CHTb in applications where waste heat between 50 and 90 °C is available and upgraded heat up to about 130 °C is required. The use of a compressor allows operation at a thermal lift not achievable with conventional heat transformer. At the same time, the CHTb can achieve a significantly higher COP_{el} than a vapor compression heat pump in most of the applications considered. Normally heat transformers are considered interesting in the cases where a large amount of waste heat is available. However, in the case of a CHTb, the increase in COP_{el} compared to a heat pump can compensate for this drawback, allowing this technology to be used in a greater number of cases. In addition, this disadvantage is completely overcome when the CHTb is used to supply heat simultaneously to a low and a high temperature district heating network, as both the high and the low temperature heat flow become useful heat. This is also the application with the highest COP_{el}.

5. Conclusions

This work presented and compared the alternative configurations of a compressor-assisted heat transformer with a compressor integrated in the absorption cycle. The two configurations differ in the position of the compressor: at low pressure, between the generator and the condenser (CHTa), and at high pressure, between the evaporator and the absorber (CHTb). The characteristics of the two configurations were investigated by means of numerical simulations. The analysis showed that, for a given operating condition, the compressor operation can be adjusted to maximize the electrical COP with little effect on the thermal COP.

The two cycle configurations have been compared assuming waste heat and heat rejection temperatures of 60 °C and 0 °C respectively, while changing the temperature of the upgraded heat from 90 °C to 120 °C. Under these conditions, the calculations showed that the CHTb can achieve a COP in the range of 5–14, while the CHTa in the range of 1.2–6. This advantage of the CHTb over the CHTa is due to:

- Lower specific volume at the compressor inlet (0.06–0.07 m^3/kg vs. 0.27–1.10 m^3/kg) and therefore lower volume flow rate handled by the compressor;
- Lower compression ratio (2.2 vs. 5.6) in the most demanding conditions, i.e. when the required contribution to the compressor is greater.
- Direct recovery of the superheat at the compressor outlet as useful heating power.

On the other hand, even if the CHTb operates at higher pressures than the CHTa, this should not be particularly challenging, as maximum pressure under the conditions studied is below 55 bar.

Due to the better performance of the CHTb, this configuration was tested in four possible applications and four operating conditions were studied for each application. The numerical results show that the CHTb is a suitable solution for the applications considered and that its COP_{el} can be significantly higher than that of a vapor compression heat pump. With more detail:

- When used in district heating networks, a COP_{el} of up to 12.5 was found, while the maximum value for a heat pump in the same condition is 6.3.
- When producing steam for industrial use, with COP_{el} from 5.0 to 6.3 against 4.2 of the heat pump for steam at 3 bar.
- When used to evaporate water in desalination plants, the CHTb had the same COP_{el} (4.5) as a heat pump in the most demanding conditions, i.e. when the heat rejection temperature is 35 °C. However, as this temperature is lowered, a COP_{el} of up to 11.6 can be found, almost the double of the 5.6 calculated for the heat pump.

These results suggest that the CHTb is a suitable heat recovery technology for upgrading heat up to about 130 °C, overcoming the temperature lift limitation of the AHT and ensuring a higher COP_{el} than a vapor compression heat pump.

Given the higher complexity compared to both AHT and heat pump, the design of a CHT will need to ensure stable operation even in the presence of fluctuating temperatures. This opens the door for further research that could assess this issue based on dynamic modelling of the system.

CRediT authorship contribution statement

Tommaso Toppi: Writing – original draft, Methodology, Formal analysis, Data curation, Conceptualization. **Gianluca Abrami:** Writing – review & editing, Formal analysis, Data curation. **Marcello Aprile:** Writing – review & editing, Validation, Conceptualization.

Declaration of competing interest

The authors declare that they have no known competing financial interests or personal relationships that could have appeared to influence the work reported in this paper.

References

Aprile, M., Toppi, T., Garone, S., Motta, M., 2018. STACY-A mathematical modelling framework for steady-state simulation of absorption cycles. Int. J. Refrig. 88, 129–140. https://doi.org/10.1016/j.ijrefrig.2017.12.019.

Arpagaus, C., Bless, F., Uhlmann, M., Schiffmann, J., Bertsch, S.S., 2018. High temperature heat pumps: market overview, state of the art, research status, refrigerants, and application potentials. Energy 152, 985–1010. https://doi.org/10.1016/j.energy.2018.03.166.

Cudok, F., Giannetti, N., Corrales Ciganda, J.L., Aoyama, J., Babu, P., Coronas, A., Fujii, T., Inoue, N., Saito, K., Yamaguchi, S., Ziegler, F., 2021. Absorption heat transformer - state-of-the-art of industrial applications. Renew. Sustain. Energy Rev. 141, 110757. https://doi.org/10.1016/j.rser.2021.110757.

Davies, G., Lagoeiro, H., Turnell, H., Wegner, M., Foster, A., Evans, J., Revesz, A., Leiper, A., Smyth, K., Hamilton, J., Cooke, H., Maidment, G., 2023. Evaluation of low

temperature waste heat as a low carbon heat resource in the UK. Applied Thermal Engineering, 235, 121283. https://doi.org/10.1016/j.applthermaleng.2023.121283.
Ebrahimi, K., Jones, G.F., Fleischer, A.S., 2014. A review of data center cooling technology, operating conditions and the corresponding low-grade waste heat recovery opportunities. Renew. Sustain. Energy Rev. 31, 622–638. https://doi.org/10.1016/j.rser.2013.12.007.
Gebreslassie, B.H., Medrano, M., Boer, D., 2010. Exergy analysis of multi-effect water-LiBr absorption systems: from half to triple effect. Renew. Energy 35 (8), 1773–1782. https://doi.org/10.1016/j.renene.2010.01.009.
Gao, J.T., Xu, Z.Y., Wang, R.Z., 2021a. Enlarged temperature lift of hybrid compression-absorption heat transformer via deep thermal coupling. Energy Convers. Manage 234, 113954. https://doi.org/10.1016/j.enconman.2021.113954.
Gao J.T., Xu Z.Y., Wang R.Z., 2021. An air-source hybrid absorption-compression heat pump with largetemperature lift, Appl. Energy 291, 116810. https://doi.org/10.1016/j.apenergy.2021.116810.
Garone, S., Toppi, T., Guerra, M., Motta, M., 2017. A water-ammonia heat transformer to upgrade low-temperature waste heat. Appl. Therm. Eng. 127, 748–757. https://doi.org/10.1016/j.applthermaleng.2017.08.082.
Hackl, R., Andersson, E., Harvey, S., 2011. Targeting for energy efficiency and improved energy collaboration between different companies using total site analysis (TSA). Energy 36, 4609–4615. https://doi.org/10.1016/j.energy.2011.03.023.
Ibrahim, O.M., Klein, S.A., 1993. Thermodynamic properties of ammonia-water mixtures. ASHRAE Trans. 21 (2), 1495.
Jiang, L., Wang, R.Q., Tao, X., Roskilly, A.P., 2020. A hybrid resorption-compression heat transformer for energy storage and upgrade with a large temperature lift. Appl. Energy 280, 115910. https://doi.org/10.1016/j.apenergy.2020.115910.
Johra, J., 2022. Overview of the Coefficient of Performance (COP) For Conventional Vapour-Compression Heat Pumps in Buildings. Department of the Built Environment, Aalborg University, pp. 1901–7286. DCE Lecture notes No. 79 ISSN.
Loni, R., Najafi, G., Bellos, E., Rajaee, F., Said, Z., Mazlan, M., 2021. A review of industrial waste heat recovery system for power generation with Organic Rankine cycle: recent challenges and future outlook. J. Clean. Prod. 287, 125070. https://doi.org/10.1016/j.jclepro.2020.125070.
Luberti, M., Gowans, R., Finn, P., Santori, G., 2022. An estimate of the ultralow waste heat available in the European Union. Energy 238, 121967. https://doi.org/10.1016/j.energy.2021.121967.
Ma, Z., Bao, H., Roskilly, A.P., 2016. Performance analysis of ultralow grade waste heat upgrade using absorption heat transformer. Appl. Therm. Eng. 101, 350–361. https://doi.org/10.1016/j.applthermaleng.2016.02.002.
Moser, S., Lassacher, S., 2020. External use of industrial waste heat - an analysis of existing implementations in Austria. J. Clean. Prod. 264, 121531. https://doi.org/10.1016/j.jclepro.2020.121531.
Mostofizadeh, C., Kulick, C., 1998. Use of a new type of heat transformer in process industry. Appl. Therm. Eng. 18, 857–874. https://doi.org/10.1016/S1359-4311(97)00115-4.
Rattner, A.S., Garimella, S., 2011. Energy harvesting, reuse and upgrade to reduce primary energy usage in the USA. Energy 36, 6172–6183. https://doi.org/10.1016/j.energy.2011.07.047.
Rivera, W., Best, R., Hernandez, J., Heard, C.L., Holland, F.A., 1994a. Thermodynamic study of advanced absorption heat transformers – I. Single and two stage configurations with heat exchangers. Heat Recov. Syst. CHP 14, 173–183. https://doi.org/10.1016/0890-4332(94)90008-6, 1994.
Rivera, W., Best, R., Hernandez, J., Heard, C.L., Holland, F.A., 1994b. Thermodynamic study of advanced absorption heat transformers – II. Double absorption configurations. Heat Recov. Syst. CHP 14 (2), 185–193. https://doi.org/10.1016/0890-4332(94)90009-4.
Toppi, T., Aprile, M., Guerra, M., Motta, M., 2016. Numerical investigation on semi-GAX NH3-H2O absorption cycles. Int. J. Refriger. 66, 169–180. https://doi.org/10.1016/j.ijrefrig.2016.02.009.
Toppi, T., Aprile, M., Guerra, M., Motta, M., 2017. Performance assessment of a double-lift absorption prototype for low temperature refrigeration driven by low–grade heat. Energy 125, 287–296. https://doi.org/10.1016/j.energy.2017.02.052.
Wang, J., Wu, W., Li, X., Wang, B., Shi, W., 2017. Analysis of a compression-assisted absorption heat transformer. Proceedings of 12th IEA Heat Pump Conference. Rotterdam, June 2017. ISBN 978-90-9030412-0.
Wang, J., Wang, B., Li, X., Wu, W., Shi, W., 2018. Performance analysis on compression-assisted absorption heat transformer: a new low-temperature heating system with higher heating capacity under lower ambient temperature. Appl. Therm. Eng. 134, 419–427.
Xu, Z.Y., Wang, R.Z., 2018. Comparison of absorption refrigeration cycles for efficient air-cooled solar cooling. Solar Energy Energy 172, 14–23. https://doi.org/10.1016/j.solener.2018.04.004.
Zhang X., Wang R.Z., Xu Z.Y., 2022. Air-source hybrid absorption-compression heat pumps with three-stage thermal coupling configuration for temperature lift over 150 °C. Energy Convers. Manage 271, 116304. https://doi.org/10.1016/j.enconman.2022.116304.
Zhao, Z., Zhou, F., Zhang, X., Li, S., 2003a. The thermodynamic performance of a new solution cycle in double absorption heat transformer using water/lithium bromide as the working fluids. Int. J. Refrig. 26, 315–320. https://doi.org/10.1016/S0140-7007(02)00114-7.
Zhao, Z., Ma, Y., Chen, J., 2003b. Thermodynamic performance of a new type of double absorption heat transformer. Appl. Therm. Eng. 23, 2407–2414. https://doi.org/10.1016/j.applthermaleng.2003.08.006.
Zhao, Z., Zhang, X., Ma, X., 2005. Thermodynamic performance of a double-effect absorption heat-transformer using TFE/E181 as the working fluid. Appl. Energy 82, 107–116. https://doi.org/10.1016/j.apenergy.2004.10.012.
Zhou, J., Liu, F., Gong, Y., Sui, J., 2024. Performance investigation of a high-temperature absorption-compression heat transformer with liquid refrigerant injection. Energy Convers. Manage 321, 119110. https://doi.org/10.1016/j.enconman.2024.119110.
Ziegler, B., Trepp, C., 1984. Equation of state for ammonia-water mixtures. Int. J. Refrig. 7 (2), 101–106. https://doi.org/10.1016/0140-7007(84)90022-7.